Archives of Virology (2024) 169:98
https://doi.org/10.1007/s00705-024-06021-7

ORIGINAL ARTICLE

Analysis of the interaction between the ORF42 and ORF55 proteins encoded by Kaposi's sarcoma-associated herpesvirus

Kazushi Kuriyama[1] · Tadashi Watanabe[1] · Shinji Ohno[1]

Received: 4 September 2023 / Accepted: 1 February 2024 / Published online: 15 April 2024

Abstract

Kaposi's sarcoma-associated herpesvirus (KSHV) causes Kaposi's sarcoma, primary effusion lymphoma, and multicentric Castleman disease. The tegument is a structure that is unique to herpesviruses that includes host and viral proteins, including the viral ORF42 and ORF55 proteins. Alphaherpesvirus tegument proteins have been well studied, but much is unknown regarding KSHV. Here, we report an interaction between the ORF42 and ORF55 proteins. ORF55 interacted with and recruited ORF42 from the nucleus to the cytoplasm. When ORF42 and ORF55 were expressed simultaneously in cultured cells, the expression level of these two viral proteins was higher than when either was expressed independently. ORF55, but not ORF42, was polyubiquitinated, suggesting that an unidentified regulatory mechanism may be present. A recombinant virus with an ectopic stop codon in ORF42 exhibited normal replication of genomic DNA, but fewer virus particles were released with the recombinant than with the wild-type virus. A unique R136Q mutation in ORF42, which is found in a KSHV strain that is prevalent on Miyako Island, Okinawa Prefecture, Japan, further increased the expression of ORF42 and ORF55 when these proteins were expressed simultaneously. However, the ORF42 R136Q mutation did not affect the localization pattern of ORF42 itself or of ORF55. In addition, experiments with a recombinant virus possessing the ORF42 R136Q mutation showed lower levels of production of the mutant virus than of the wild-type virus, despite similar levels of genome replication. We suggest that the R136Q mutation in ORF42 plays an important role in ORF55 protein expression and virus production.

Introduction

Kaposi's sarcoma-associated herpesvirus (KSHV), also known as human herpesvirus 8, belongs to the species *Rhadinovirus humangamma8* of the subfamily *Gammaherpesvirinae*, family *Orthoherpesviridae* [1]. This virus infects various cell types *in vivo*, including B lymphocytes, monocytes, endothelial cells, epithelial cells, and keratinocytes, and causes Kaposi sarcoma, primary effusion lymphoma, and multicentric Castleman disease [2–5]]. KSHV has a double-stranded DNA genome containing more than 90 open reading frames (ORFs) and encoding various microRNAs [5].

KSHV, like other herpesviruses, exhibits two phases of infection in its replication cycle: latent and lytic. In the latent phase, the KSHV genome is maintained as a non-integrated extrachromosomal episome in the nucleus of infected cells without virus production [6]. Only a limited number of genes, including those encoding latent nuclear antigen, vCyclin, and viral FLICE inhibitory protein, are expressed. These genes play a role in maintaining the latent state and are called "latency-associated genes".

Various stimuli induce the expression of the viral transactivator encoded by ORF50 and trigger the lytic phase of infection. In this phase, almost all the viral genes are activated. According to their temporal expression patterns, genes are classified into three categories: immediate early (IE), early (E), and late (L). IE genes encode transactivators such as the ORF50 protein, E genes encode the viral polymerase and related proteins, which contribute to viral genome replication, and L genes encode structural proteins that make up the KSHV virion [5, 7–9].

Herpesvirus virions consist of a genome, capsid, tegument, and envelope. The viral genome is enclosed in the

Handling Editor: Akbar Dastjerdi

✉ Shinji Ohno
soono@med.u-ryukyu.ac.jp

[1] Department of Virology, Graduate School of Medicine, University of the Ryukyus, 207 Uehara, Nishihara, Nakagami, Okinawa 903-0215, Japan

capsid shell to constitute the nucleocapsid core, which is further wrapped with an envelope from which various viral glycoproteins are extruded. The area between the nucleocapsid and envelope is called the tegument and is unique to herpesviruses. Various cellular and viral proteins are present in this region [10, 11]. The ORF42 and ORF55 gene products are considered tegument proteins; however, their functions remain to be elucidated. Using an ORF42-deficient recombinant virus with an ectopic stop codon in the ORF42 gene, Butnaru et al. demonstrated that the ORF42 protein has the ability to modulate the expression of various genes, including immediate-early, early, and late genes, to some extent [12]. They also demonstrated that ORF42 is exclusively present in the cytoplasm and is required for intracellular virion production [12]. The viral Bcl-2 homolog (vBcl2) of KSHV binds to the ORF55 protein and is involved in the incorporation of the ORF55 protein into virions [13], suggesting that ORF55 could be a key protein for viral particle formation.

Mammalian herpesviruses have about 40 genes in common, termed "core genes" and these are believed to have been inherited from a common ancestor [14]. ORF42 and ORF55 are core genes that are expressed as L genes [9, 14]. Herpes simplex virus (HSV)-1 UL7 and Epstein-Barr virus (EBV) BBRF2 are homologs of KSHV ORF42, whereas HSV-1 UL51 and EBV BSRF1 are homologs of KSHV ORF55 [15]. Both UL51 and BSRF1 are palmitoylated and membrane-associated [16, 17]. HSV-1 UL51 binds to UL7 and glycoprotein E and recruits them to the cytoplasmic membrane [18]. EBV BBRF2 complexes with BSRF1. Deletion of BBRF2 reduces viral infectivity [19].

The ORF42 and ORF55 proteins of KSHV exhibit limited sequence similarity to their homologs in EBV, BBRF2, and BSRF1, with 35.8% and 46.4% amino acid sequence identity, respectively, although EBV and KSHV both belong to the subfamily *Gammaherpesvirinae*. We therefore investigated whether these two proteins have the same function(s) as their homologs in other herpesviruses. We found that ORF55 interacts with and affects the cellular localization of ORF42. Furthermore, using a recombinant virus lacking ORF42, we confirmed that ORF42 is necessary for efficient production of virus particles. These observations provide insights into the functions of ORF42 and ORF55 during viral infection.

Materials and methods

Cell culture and reagents

293T and HeLa cells were cultured in DMEM containing 10% fetal bovine serum and penicillin/streptomycin (growth medium). iSLK cells were cultured in growth medium containing 1 μg of puromycin (FUJIFILM Wako) and 250 μg of G418 (Nacalai Tesque) per mL. Mouse anti-FLAG monoclonal antibody (mAb; clone 1E6: FUJIFILM Wako), mouse anti-HA mAb (clone 4B2; FUJIFILM Wako), rabbit anti-HA polyclonal antibody (pAb; Proteintech: 51064-2-AP), rabbit anti-ubiquitin pAb (GeneTex: GTX128826), and mouse anti-beta-tubulin mAb (clone 10G10; FUJIFILM Wako) were purchased. Polyethyleneimine (PEI MAX, MW 40,000; Polysciences) was dissolved at a concentration of 2 mg/mL in distilled water, filter-sterilized, and used for plasmid transfection.

Plasmids

The expression plasmid pCI-blast has been described previously [20]. pCI-blast-FLAG-ORF42, pCI-blast-HA-ORF55, and pCI-blast-FLAG-ORF55 were generated using PCR by BCBL-1 DNA as template. Truncation mutants of ORF42 were obtained using overlap extension PCR. The primers used in this study are listed in Table 1.

Coprecipitation and immunoblotting

Expression plasmids were transfected using PEI MAX. Transfected cells were harvested at 24 h post-transfection by scraping with cold phosphate-buffered saline (PBS). Cell pellets were resuspended in lysis buffer (10 mM Tris, pH 7.5, 150 mM NaCl, 0.5 mM EDTA, 0.5% NP-40, and 1% (v/v) EDTA-free protease inhibitor cocktail [Nacalai Tesque]) and incubated on ice for 30 min. The sample was then centrifuged at 20,000 × *g* at 4°C for 30 min, and the supernatant was collected. Mouse anti-FLAG or mouse anti-HA mAb and protein A-agarose beads (Santa Cruz Biotechnology) were added to the supernatants, and the mixtures were incubated with rotation at 4°C. After incubation, the beads were washed five times with lysis buffer without the protease inhibitor cocktail. The supernatant was removed, and the beads were resuspended in sodium dodecyl sulfate-polyacrylamide gel electrophoresis (SDS-PAGE) loading buffer and boiled for 5 min. Samples were separated by SDS-PAGE in 10% or 12.5% polyacrylamide gels and transferred onto polyvinylidene fluoride membranes. Subsequently, the membranes were blocked with PBS containing 0.1% Tween-20 (PBS-T) and 5% (w/v) non-fat milk powder for 1 h at room temperature and then incubated with the primary antibody (1:1000) for 1 h at room temperature. After washing with PBS-T, the blots were incubated with a horseradish peroxidase-conjugated secondary antibody (1:10,000) for 1 h at room temperature. The membrane was treated with EzWestLumi plus (ATTO), and the chemiluminescent signal was exposed to an X-ray film (FUJIFILM Wako). The developed X-ray film was scanned, and ImageJ software (version 1.54 d) was used to quantify the signal intensity.

Table 1 Primers used in this study

Purpose and name	Sequence (5'→3')
BAC mutagenesis[a]	
S_ORF42-stop-EP	ccaccctgtggtgccccgccttgtcctggaagtgcataggTaaaacaacgcactggttggaTAGGGATAACAGGGTAATCGATTT
As_ORF42-stop-EP	gacattttgggggtattgcttccaaccagtgcgttgttttAcctatgcacttccaggacaaGCCAGTGTTACAACCAATTAACC
S_ORF42-R136Qmyk-EP	accgagctctgctgcctgttatcgatgctcgagaactgtcAagacatgtcaccaacgttttTAGGGATAACAGGGTAATCGATTT
As_ORF42-R136Qmyk-EP	gcgactaataatagatctcaaaaacgttggtgacatgtctTgacagttctcgagcatcgatGCCAGTGTTACAACCAATTAACC
Cloning expression plasmid[b]	
2S_EcoRI_FLAG_KSHV-ORF42	catgaattcATGGATTACAAGGACGACGATGACAAGatgtccctggaaaggg
As_KSHV-ORF42_NotI	caaaataagcggccgcttattttgaaaaaagggaaacaatg
S_EcoRI_KSHV-ORF55	catgaattcatgtcgtctccatggtacac
As_KSHV-ORF55_HA_XhoI	tagctcgagctaTGCATAATCCGGAACATCATACGGATAtgtcgaacctatcgcg
S_EcoRI_FLAG_KSHV ORF55	catgaattcATGGATTACAAGGACGACGATGACAAGatgtcgtctccatggtac
As_KSHV ORF55_NotI	gcggccgcttatgtcgaacctatcgcgctttc
ORF42 truncated mutant construction[b]	
As_A1_KSHV ORF42_NotI	ttgcggccgcttactccaccaggc
S_EcoRI_FLAG_ORF42_del(1-279)	catgaattcATGGATTACAAGGACGACGATGACAAGcacgaagacatggtgac
As_ORF42_del(559-837)_SalI	cgattaagtcgacttaatcgtccacggacagct
S_A3_EcoRI_FLAG_KSHV ORF42	catgaattcATGGATTACAAGGACGACGATGACAAGcatttcagggccac

[a]Lowercase indicates a sequence with homology to the KSHV BAC16 sequence, underlined uppercase indicates a mutagenesis site, and uppercase indicates the pEP-KanS squence.

[b]Underlined lowercase indicates a restriction enzyme site, and uppercase indicates the tag protein sequence.

Protein degradation assay

Plasmids for expression of FLAG-ORF42 or FLAG-ORF55 were introduced by transfection into 293T cells. The cells were treated with or without 10 μM MG132, a proteasome inhibitor, for 3 h, and the culture medium was replaced with medium containing 10 μM MG132 and 50 μM cycloheximide (CHX). At 0, 2, 4, and 6 h after CHX treatment, protein samples were prepared as above.

Immunofluorescence assays

HeLa cells seeded on glass slides were transfected with expression plasmids using PEI-MAX. One day after transfection, the cells were washed with PBS and fixed with methanol for 5 min at room temperature. The cells were then incubated with an anti-FLAG pAb and/or anti-HA mAb. After washing, the cells were incubated with Alexa Fluor 488– or fluorescein isothiocyanate–conjugated anti-mouse IgG and Alexa Fluor 594–conjugated anti-rabbit IgG. Nuclei were stained with DAPI using ProLong Glass Antifade Mountant with NucBlue (Thermo Fisher Scientific). Immunofluorescent images were obtained using an inverted confocal microscope (Nikon C2; Nikon).

Mutagenesis of KSHV BAC16

KSHV BAC16 (accession number: GQ994935) was kindly provided by Jae U. Jung, and KSHV BAC16 mutagenesis was performed according to the developer's protocols [21]. Nucleotide positions for mutagenesis were according to GenBank accession no. GQ994935. The primers used for mutagenesis are listed in Table 1. The insertion and deletion of kanamycin-resistance cassettes (Kan^R) in each mutant were analyzed by digestion with KpnI and agarose gel electrophoresis. The mutations in each BAC clone were confirmed by Sanger sequencing.

Establishment of doxycycline-inducible recombinant KSHV-expressing cells

To obtain efficient recombinant KSHV-producing cells, tetracycline/doxycycline (Dox)-inducible (Tet-on) RTA/ORF50-expressing SLK cells (iSLK) were used. KSHV wild-type BAC16 (WT-BAC16) and mutants (ORF42 STOP-BAC16 and ORF42 R136Q-BAC16) were introduced into iSLK cells by transfection, using the calcium phosphate method. The transfected cells were treated with 1000 μg of hygromycin B (FUJIFILM Wako) per mL to select Dox-inducible, recombinant KSHV-producing cell lines (iSLK-WT, iSLK-ORF42 STOP, and iSLK-ORF42 R136Q cells).

Measurement of virus production and viral DNA replication

To evaluate virus production, the KSHV genome in the culture supernatant was quantified as described previously [22–24]. Briefly, iSLK cells (iSLK-WT, iSLK-ORF42 STOP, and iSLK-ORF42 R136Q cells) were treated with 0.75 mM sodium butyrate (NaB) and 4 μg of Dox per mL for 72 h to induce lytic replication of recombinant KSHV, and the culture supernatants were harvested. The supernatants (150 μL) were treated with DNase I (New England Biolabs) to obtain only enveloped and encapsidated viral genomes. Total DNA was extracted from 100 μL of the DNase-I-treated culture supernatant using a QIAamp DNA Blood Mini Kit (QIAGEN). For quantification of the viral DNA, SYBR Green real-time PCR was performed using KSHV-encoded ORF11-specific primers. The values obtained were normalized to the sample volume. To measure genome replication, iSLK cells were treated with Dox and NaB for 48 h to induce lytic replication. Total cellular DNA was extracted using a QIAamp DNA Blood Mini Kit. The number of cellular KSHV genome copies was determined using SYBR Green real-time PCR and normalized to the amount of DNA used for the real-time PCR.

Results

ORF42 forms a complex with ORF55

Viruses of the family *Herpesviridae* share 43 "core genes" believed to be inherited from a common ancestor. KSHV ORF42 and ORF55 are core genes [14]. The amino acid sequence of KSHV ORF42 is 35.8% identical to that of EBV BBRF2, and that of KSHV ORF55 is 46.6% identical to that of BSRF1. KSHV and EBV are members of the subfamily *Gammaherpesvirinae*, and the amino acid sequence similarity in these proteins is the highest among the human herpesviruses. Previous reports have shown that the homologs of KSHV ORF42 (HSV-1 UL7 and EBV BBRF2) interact with those of ORF55 (HSV-1 UL51 and EBV BSRF1) [19, 25]. Therefore, we examined whether ORF42 interacts with ORF55, using a co-immunoprecipitation assay (Fig. 1). As shown in Fig. 1, a C-terminally HA-tagged ORF55 was efficiently coprecipitated with an N-terminal FLAG-tagged ORF42. Unexpectedly, multiple HA-ORF55 bands were observed, some corresponding to a higher molecular weight than predicted for the full-length protein. These data suggest that KSHV ORF42 and ORF55 form complexes similar to those of other herpesviruses [19, 25].

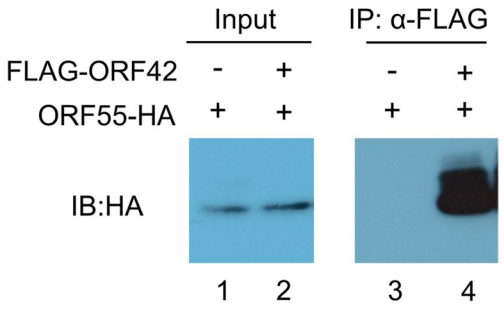

Fig. 1 Interaction of ORF42 with ORF55. FLAG-tagged ORF42 and HA-tagged ORF55 were expressed in 293T cells. Immunoprecipitation was performed using an anti-FLAG mAb, and the precipitates were analyzed by SDS-PAGE and immunoblot assay. Representative data from three independent experiments are presented

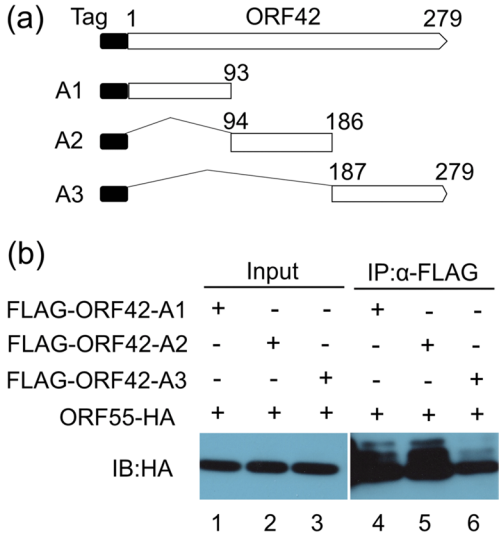

Fig. 2 Binding of ORF55 with multiple parts of ORF42. (**a**) Schematic illustration of the ORF42 truncation mutants. (**b**) FLAG-tagged ORF42 truncation mutants were expressed together with HA-tagged ORF55 in 293T cells. The cell lysates were used for immunoprecipitation assay using an anti-FLAG antibody, and the precipitates were analyzed by SDS-PAGE and immunoblot assay. Representative data from three independent experiments are presented

ORF42 associates with ORF55 via multiple parts

To investigate which part of ORF42 is necessary for interaction with ORF55, we divided ORF42 into three parts, tagged each with a FLAG epitope at its N-terminus (Fig. 2a), and examined its interaction with ORF55 using a co-immunoprecipitation assay. All of the mutants were coprecipitated with FLAG-ORF55 (Fig. 2b, lanes 4-6), although the A3 mutant was co-immunoprecipitated with ORF55 with low efficiency. Signals above the main signals of ORF55, which were most significant in A2, were also detected. The data showed that ORF42 binds to ORF55 in more than three parts.

ORF42 and ORF55 mutually increase protein expression

The signal intensity of ORF42 in the immunoblot analysis increased in the presence of ORF55. To compare the signal differences, the developed X-ray films were scanned, and the signal intensities were quantified using ImageJ software. When both proteins were expressed simultaneously, the signal intensities for ORF42 and ORF55 were approximately 3 and 1.5 times higher, respectively, than when each was expressed alone (Fig. 3a). Interestingly, upregulation of ORF55 expression was not observed when ORF42 truncation mutants were expressed simultaneously (Fig. 3b), indicating that full-length ORF42 is required for regulation of ORF55 expression. The A3 mutant was almost undetectable in the immunoblotting assay (Fig. 3b, lane 4, middle panel).

The ubiquitin-proteasome pathway is involved in protein degradation. To determine whether this pathway contributed to the difference in protein expression, we examined protein ubiquitination (Fig. 3c). Polyubiquitination was observed with ORF55 but not with ORF42. No polyubiquitination of ORF42 was observed, even after treatment with MG132, a proteasome inhibitor (data not shown).

MG132 stabilized ORF55 slightly after 6 h of treatment with CHX and MG132, indicating that the degradation of ORF55 was ubiquitin-dependent (Fig. 4a). Surprisingly, the proteasome inhibitor stabilized Flag-ORF42 significantly (Fig. 4b), indicating that ORF42 was degraded by proteasomes. A small number of cellular proteins are under the control of ubiquitin-independent proteasomal degradation [26]. As we could not detect polyubiquitinated ORF42, this protein might be degraded by an unusual mechanism.

ORF42 is recruited to the cytoplasm by ORF55

Previous reports have indicated that the presence of the corresponding ORF55 homologs (HSV-1 UL51 or EBV BSRF1) causes relocation of the ORF42 homologs (HSV-1 UL7 or EBV BBRF2) to the Golgi apparatus [16, 19, 25]. Therefore, we examined the intracellular localization of these proteins using immunofluorescence microscopy. When expressed independently, ORF42 was localised in the cytoplasm and nucleus, and a granule-like fluorescence pattern was seen in the nucleus. For ORF55, a major proportion of the protein was located in the cytoplasm, particularly in the perinuclear area (Fig. 5). The localization patterns of the two proteins were concordant with those reported previously [27]. We conclude that the distribution of ORF42 is altered in the presence of ORF55, that the majority of ORF42 colocalizes in the cytoplasm with ORF55, and that a small fraction of ORF42 remains in the nucleus.

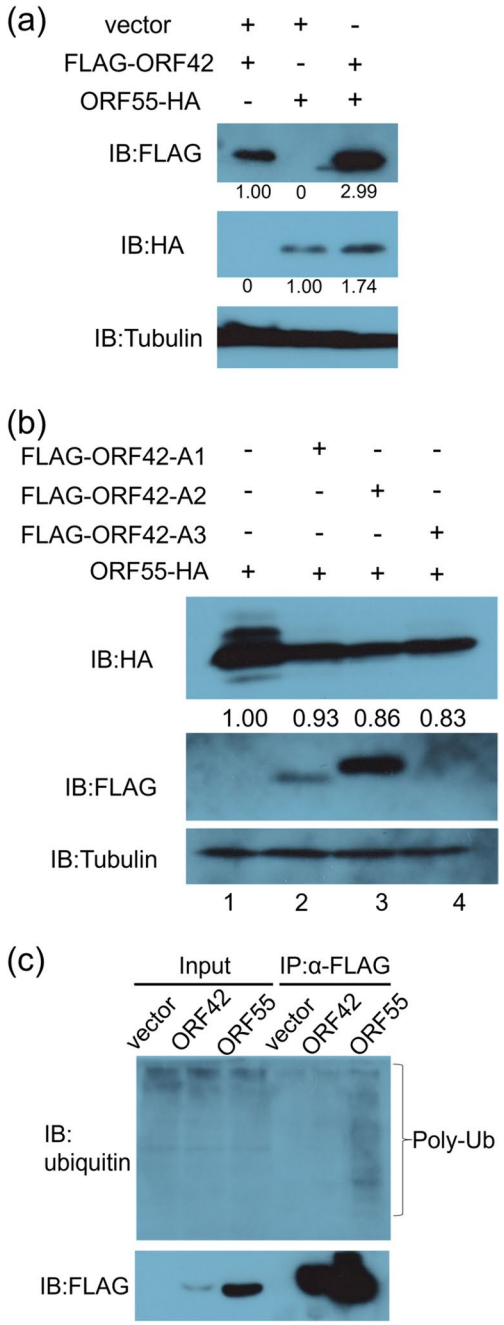

Fig. 3 Effect of ORF42 and ORF55 interactions on protein expression levels. (**a**) Effect of coexpression. Cells were transfected with the indicated plasmids (1 μg each) and subjected to immunoblot analysis the following day. The intensity of the signal was quantified using ImageJ software and normalized to the tubulin signal. Signal intensities of ORF42 and ORF55 expressed alone were set to 1.0. (**b**) Effect of truncation mutations. FLAG-tagged ORF42 truncation mutants were expressed together with HA-tagged ORF55 in 293T cells. Protein expression was analyzed by immunoblot and quantified. The signal intensity of ORF55 expressed alone was set to 1.0. (**c**) Detection of poly-ubiquitination signals. FLAG-tagged ORF42 or ORF55 was expressed in 293T cells. The proteins were immunoprecipitated, separated by SDS-PAGE, and analyzed using an immunoblot assay. Representative data from three independent experiments are presented

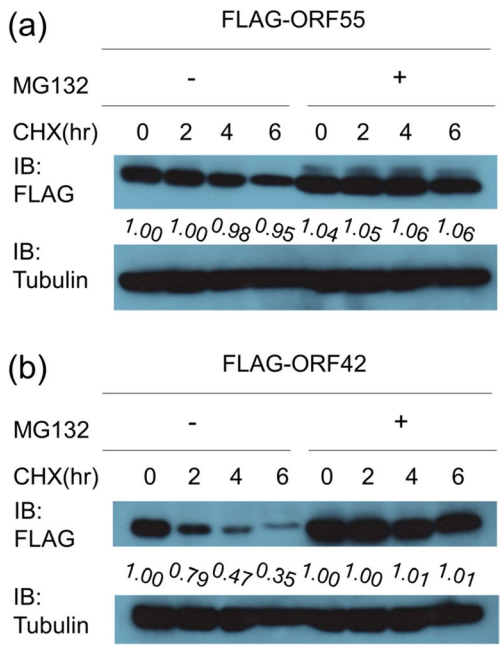

Fig. 4 Degradation kinetics of FLAG-ORF55 and FLAG-ORF42. (**a**) and (**b**) FLAG-tagged ORF55 (**a**) or FLAG-tagged ORF42 (**b**) was expressed in 293T cells. After 3 h of treatment with MG132, the cells were cultured in the presence of CHX and MG132. At the indicated time points of CHX treatment, protein samples were prepared, analyzed by immunoblot, and quantified. The signal intensity of ORF42 or ORF55 for cells not treated with MG132 and CHX was set to 1.0

The mutation R136Q in ORF42 increases the expression of both the ORF42 and ORF55 proteins

Eighteen percent of the inhabitants of Miyako Island, Okinawa Prefecture, Japan, who are over 50 years old are positive for KSHV, and the incidence of Kaposi's sarcoma in people over 50 years of age in this area is around 1,000 times higher than that in mainland Japan [28]. The R136Q mutation in ORF42 is unique to KSHV from Miyako Island [28]. We therefore tested whether this mutation in ORF42 affects its interaction with ORF55. As shown in Fig. 6a, the ORF42 R136Q mutant was able to bind to ORF55. Next, we compared the protein expression level of ORF55 coexpressed with wild-type ORF42 or ORF42 R136Q and also compared the expression levels of wild-type ORF42 and ORF42 R136Q when coexpressed with ORF55 (Fig. 6b). The data suggest that ORF42 R136Q stabilizes ORF55 and itself more efficiently than wild-type ORF42. Subsequently, we investigated whether the R136Q mutation affects the intracellular localization of ORF42 and ORF55. When expressed alone, the R136Q mutant was located in the nucleus and cytoplasm with a granule-like appearance (Fig. 6b). In the presence of ORF55, the ORF42 mutant was mostly excluded from the nucleus and colocalized with ORF55 (Fig. 6c). The localization patterns of ORF55 and ORF42 R136Q were almost identical to those of the wild-type ORF42 (Fig. 5).

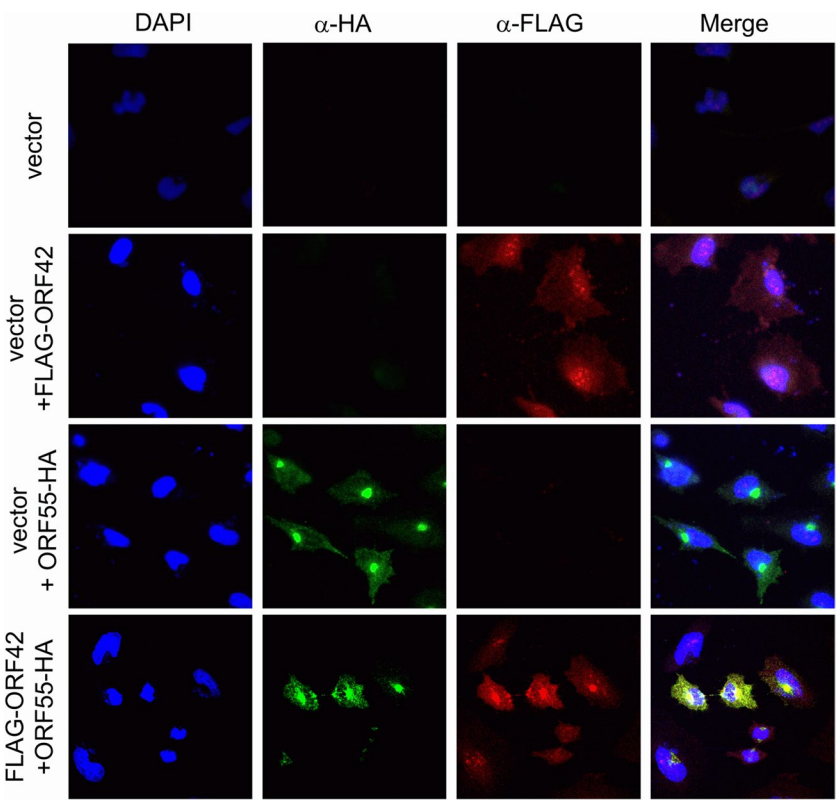

Fig. 5 Subcellular localisation of ORF42 and ORF55 in HeLa cells. HeLa cells were transfected with the indicated expression plasmids, fixed at one day post-transfection, stained with anti-FLAG (red) and anti-HA (green) antibodies and DAPI (blue) and visualized by confocal laser microscopy at 60× magnification. Representative data from three independent experiments are presented

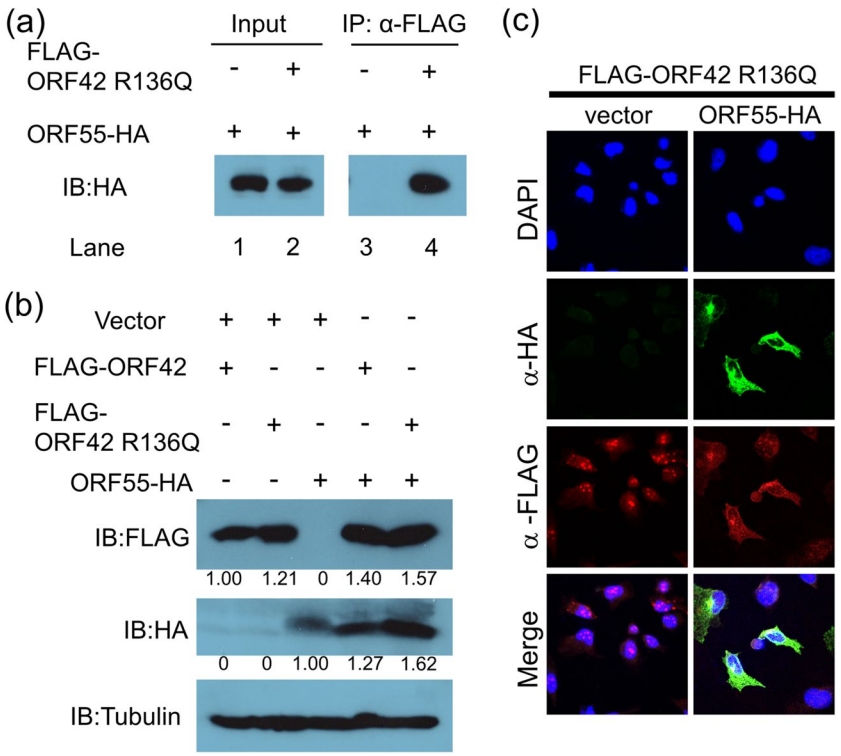

Fig. 6 Characterisation of the R136Q mutation in ORF42. (**a**) Expression of FLAG-tagged ORF42 R136Q and HA-tagged ORF55 in 293T cells. Immunoprecipitation was performed using an anti-FLAG mAb. The precipitates were analyzed by immunoblot assay. Representative data from three independent experiments are presented. (**b**) Enhancement of ORF42 and ORF55 protein expression by the R136Q mutation. Whole-cell lysates of 293T cells transfected with expression plasmids were analyzed SDS-PAGE and immunoblot assay. The levels of the ORF42 and ORF55 proteins increased if ORF42 had the R136Q mutation. (**b**) Subcellular localization of ORF42 R136Q and ORF55 in HeLa cells. HeLa cells were transfected with the indicated expression plasmids, fixed at one day post-transfection, stained with anti-FLAG (red) and anti-HA (green) antibodies and DAPI (blue) and visualized by confocal laser microscopy at 60× magnification. Representative data from three independent experiments are presented

These data suggest that the ORF42 R136Q mutant, with or without ORF55, is similar to wild-type ORF42 in its intracellular localization pattern.

Construction of ORF42-deficient and ORF42 R136Q KSHV BAC

To elucidate the role of ORF42 and the effect of the R136Q mutation in ORF42 on viral replication, we constructed a recombinant virus using KSHV BAC16, i.e., ORF42 STOP-BAC16 and ORF42 R136Q-BAC16, using a two-step markerless red recombination system [21, 29] (Fig. 7a). For ORF42 STOP-BAC16, adenine (nt 62,949) was replaced by thymine to introduce an ectopic stop codon, which resulted in the generation of immature ORF42 polypeptides. To generate ORF42 R136Q-BAC16, the arginine codon at position 136 (nt 62,681-62,683) was converted to glutamine. Insertions and deletions of the kanamycin resistance gene (Kan^R) were detected by KpnI digestion (Fig. 7b). The mutations were confirmed using Sanger sequencing (Fig. 7c).

Profiling of ORF42-deficient and ORF42 R136Q KSHV-producing cells

To efficiently induce recombinant KSHV, tetracycline/Dox-inducible (Tet-on) RTA/ORF50- expressing SLK cells (iSLK) were used as the virus-producing cells [20]. iSLK cells harboring KSHV BAC16 did not produce infectious viruses without stimulation. Upon treatment with Dox and NaB, however, the lytic cycle was triggered to produce infectious viruses.

We generated iSLK-WT, iSLK-ORF42 STOP, and iSLK-ORF42 R136Q, which were stably transfected with KSHV BAC, ORF42 STOP-BAC16, and ORF42 R136Q-BAC16, respectively. These three cell lines were treated with Dox and NaB to induce lytic infection, and this resulted in a strong increase in replication of the viral genome, with the normalized genomic copy numbers being similar in the three iSLK cell lines (Fig. 8a). This indicated that the absence of ORF42 did not affect genome replication.

Subsequently, we measured the amount of recombinant virus in the culture supernatant of the stimulated cells.

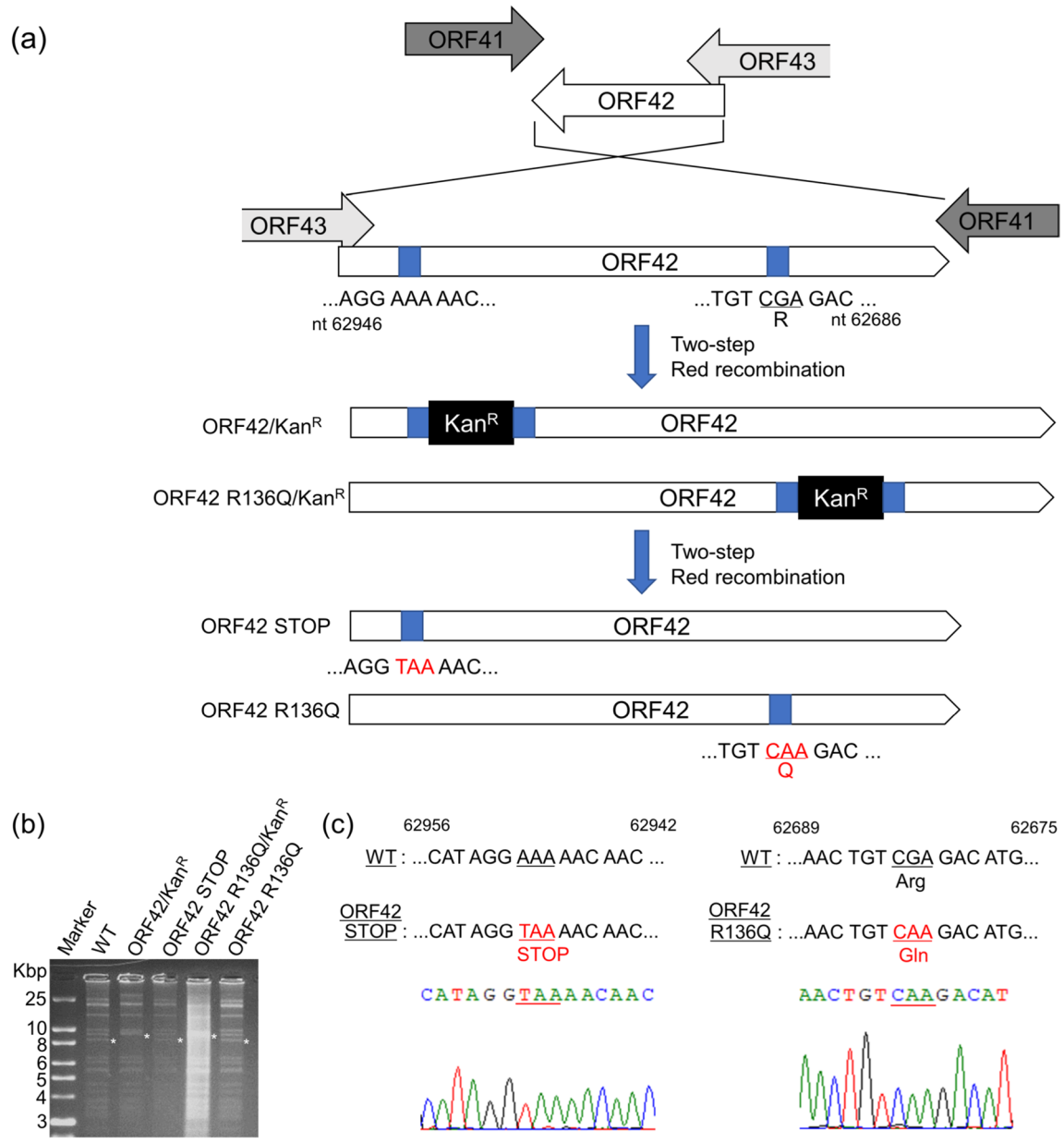

Fig. 7 Mutagenesis scheme and construction of ORF42 STOP-BAC16 and ORF42 R136Q-BAC16 based on KSHV BAC16 WT, using a two-step red recombination system. (**a**) Schematic illustration of the KSHV genome, showing the ORF42 coding region. For mutagenesis of ORF42 STOP-BAC16, the adenine at nt 62,949 was changed to thymine to introduce an ectopic stop codon. For the generation of ORF42 R136Q-BAC16, the codon for arginine 136 (nt 62,681–62,683) was replaced with a glutamine codon. (**b**) Electrophoretic pattern of the recombinant KSHV BAC DNA digested with KpnI. The asterisks (*) indicate the insertion and deletion of a kanamycin-resistance cassette in each BAC clone. (**c**) DNA sequencing results for ORF42 mutagenesis sites in ORF42 STOP-BAC16 and ORF42 R136Q-BAC16

The supernatant was treated with DNase I, total DNA was harvested from the supernatant, and genomic DNA was quantified using real-time PCR. DNA that was resistant to DNase I treatment was considered to have originated from infectious viral particles. The genome copy number of the ORF42-deficient virus in the supernatant was approximately 4% of that of the parental virus. Moreover, the amount of ORF42R136Q virus in culture supernatant was approximately 15% of that of the parental virus (Fig. 8b).

The lack of ORF42 did not affect genome replication but reduced the amount of virus produced, suggesting that this protein contributes to virus assembly. The R136Q mutation exhibited similar effects on both genome replication and virus production, although its effect on virus

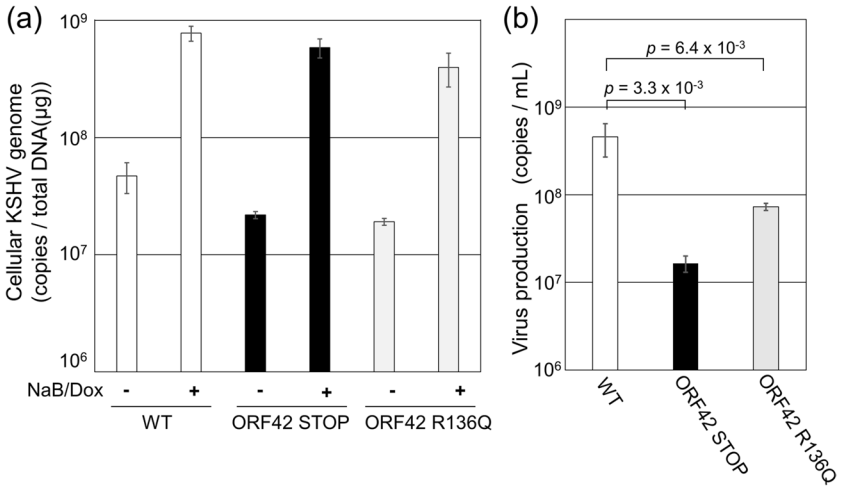

Fig. 8 Profiling of ORF42-deficient and ORF42 R136Q KSHV-producing cells. (**a**) KSHV DNA replication in iSLK-WT (WT), -ORF42 STOP (ORF42 STOP), and -ORF42 R136Q (ORF42 R136Q) cells. The cells were cultured for 48 h with a medium containing NaB and Dox. Total DNA was purified from each cell line. The number of KSHV genome copies was determined using real-time PCR and normalized to the total amount of DNA. (**b**) Virus production in iSLK cells. Each cell line was cultured for 72 h in a medium containing NaB and Dox. DNase-I-resistant DNA was purified from the culture supernatants, and the number of KSHV genome copies was determined using real-time PCR. The values obtained were normalized to the sample volume. Error bars indicate the standard deviation. Representative data from three independent experiments are presented

production was milder than that observed when no ORF42 was produced.

Discussion

Members of the family *Herpesviridae* have several "core genes" in common. KSHV ORF42 is a homolog of HSV-1 UL7 and EBV BBRF2, and KSHV ORF55 is a homolog of HSV-1 UL51 and EBV BSRF1. Like their homologs, we found that these two proteins of KSHV interact with each other. When expressed alone, KSHV ORF42 was located in the nucleus and the cytoplasm, but when coexpressed with ORF55, it was relocated from the nucleus to the cytoplasm. Previous studies have shown that the homologs of KSHV ORF42 and ORF55 accumulate in the Golgi apparatus and play a role in secondary viral envelopment [19, 25] and that HSV-1 UL7, EBV BBRF2, and KSHV ORF42 are not absolutely essential for virus replication but are necessary for efficient replication [12, 19, 30]. Butnaru et al. showed that cells infected with an ORF42-deficient recombinant virus released fewer infectious virions than those infected with the wild-type virus and that ORF42 was required for efficient production of intracellular virions [12]. In this study, we also observed that cells infected with the ORF42 STOP virus released less DNase-resistant DNA into the culture medium than those infected with wild-type virus. Although an ORF42-deficient recombinant virus with a nonsense mutation in ORF42 at serine position 25 was shown in a previous study to express early genes such as ORF6, ORF59, and ORF68 at slightly lower levels [12], this did not appear not the cause of the lower production of cell-free viral genome of the ORF42-deficient recombinant virus [12]. Because the previously investigated ORF42-deficient recombinant virus and our ORF42 STOP virus exhibited levels of intracellular genomic DNA replication similar to that of the wild-type (Fig. 8), ORF42 appears to be dispensable for viral genome replication. Considering that ORF42 is expressed late in infection [9], it is expected to play a role in virion assembly. Although ORF42 was exclusively expressed in the cytoplasm in virus-infected cells [12], a small amount of ORF42 accumulated in the nucleus when ORF42 and ORF55 were coexpressed by plasmid transfection (Fig. 5). This discrepancy might have been due to protein overexpression using a strong promoter. Taking these observations into consideration, KSHV ORF42 and ORF55 might play roles similar to those of their homologs. ORF55 also binds to vBcl2, and this interaction plays a role in the incorporation of ORF55 into virions [13]. Given that the vBcl2 homolog is conserved only among members of the subfamily *Gammaherpesvirinae*, the process of viral particle formation in KSHV- and EBV-infected cells could be different from that in HSV-1-infected cells.

In addition to HSV-1 UL7, HSV-1 UL51 interacts with glycoprotein gE. A recombinant HSV-1 lacking most of UL51 was shown to produce smaller plaques than viruses lacking gE [31]. This observation suggested that HSV-1 UL51 may have other functions that affect virion production. Because members of the subfamily *Gammaherpesvirinae* do not have a gE gene, it is not known whether the function of

KSHV ORF55 is similar to that of HSV-1 UL51. Furthermore, Oda et al. reported that HSV-1 UL14, a component of the viral pre-initiation complex, is a binding target of HSV-1 UL51 [32], suggesting that HSV-1 UL51 could affect late gene expression.

When expressed simultaneously, the levels of the KSHV ORF42 and ORF55 proteins were significantly higher than when expressed alone. ORF55 was found to be polyubiquitinated, whereas ORF42 was not. In general, polyubiquitinated proteins are degraded by proteasomes. However, the interaction between these two proteins might prevent polyubiquitinated ORF55 from undergoing proteasomal degradation. This interaction might also stabilize ORF42, accounting for its strong signal in immunoblot analysis. When the ORF42 truncation mutants and ORF55 were expressed simultaneously, none of the ORF42 mutants showed increased expression levels of ORF55. This suggests that full-length ORF42 is required for the increased expression of ORF55. Considering that we could not detect polyubiquitinated ORF42, ORF55 might have a quality control function that operates by a proteasome-independent mechanism. A small number of cellular proteins are known to be ubiquitin-independent substrates of proteasomes [26], and further studies might clarify whether this is true of ORF42. Butnaru et al. reported that ORF42 affects viral gene expression in a post-transcriptional manner [12], and it is possible that this unknown mechanism could account for the enhancement of ORF55 expression. The regulatory function of ORF42 is more apparent at later time points, and on late genes. It has been reported previously that the expression levels of some early and late genes in cells infected with an ORF42-deficient virus at day 6 after lytic cycle induction are less than half of those in cells infected with the wild-type virus [12]. The significant reduction in the expression of several viral genes might be another cause of replication failure of ORF42-deficient virus at later time points in the lytic phase.

It has been reported that a KSHV strain that is prevalent on Miyako Island in Japan has an R136Q substitution in ORF42. This mutant retains the ability to interact with ORF55 and to be relocated from the nucleus to the cytoplasm when coexpressed with ORF55. Considering that this substitution resulted in enhanced ORF55 expression, the R136Q substitution might enhance the affinity of binding of ORF42 to ORF55. This led us to expect that this substitution would enhance virus production, but, on the contrary, the ORF42 R136Q mutant produced much less virus than the parental virus, indicating that the mutation had an overall negative effect on virus production.

Acknowledgements The BAC16 KSHV clone was a gift from Kevin Brulois and Jae U. Jung (USC, USA). We thank Gregory A. Smith (Northwestern University, USA) for *Escherichia coli* strain GS1783, and Nikolaus Osterrieder (Cornell University, USA) for the plasmid pEP-KanS. K.K. was supported by a Nagai Memorial Research Scholarship from the Pharmaceutical Society of Japan. We would like to thank Editage (www.editage.jp) for English language editing.

Author contributions All authors contributed to the study conception and design. Experiments were conducted by Kazushi Kuriyama and Tadashi Watanabe. All authors interpreted the data. Kazushi Kuriyama wrote, and all authors commented on, the first draft of the manuscript. All authors read and approved the final manuscript.

Funding This study was supported by a research grant from the Okinawa Medical Science Research Foundation (to Kazushi Kuriyama).

Data availability No publicly available datasets were included in this study.

Declarations

Ethical approval Experiments using human or animal subjects were not included.

Conflict of interest The authors declare no conflict of interest.

References

1. Krug LT, Pellet PE (2022) The family Herpesviridae: A Brief introduction. In: Knipe DM, Howley PM, Damania BA, Cohen JI (eds) Fields Virology, vol 2, 7th edn. Lippincott Williams & Wilkins, pp 212–234
2. Chang Y, Cesarman E, Pessin MS, Lee F, Culpepper J, Knowles DM, Moore PS (1994) Identification of herpesvirus-like DNA sequences in AIDS-associated Kaposi's sarcoma. Science 266:1865–1869. https://doi.org/10.1126/science.7997879
3. Soulier J, Grollet L, Oksenhendler E, Cacoub P, Cazals-Hatem D, Babinet P, d'Agay MF, Clauvel JP, Raphael M, Degos L et al (1995) Kaposi's sarcoma-associated herpesvirus-like DNA sequences in multicentric Castleman's disease. Blood 86:1276–80. https://doi.org/10.1182/blood.V86.4.1276.bloodjournal8641276
4. Nador RG, Cesarman E, Chadburn A, Dawson DB, Ansari MQ, Sald J, Knowles DM (1996) Primary effusion lymphoma: a distinct clinicopathologic entity associated with the Kaposi's sarcoma-associated herpes virus. Blood 88:645–56. https://doi.org/10.1182/blood.V88.2.645.bloodjournal882645
5. Damania BA, Cesarman E (2022) Kaposi's Sarcoma Herpesvirus. In: Knipe DM, Howley PM, Damania BA, Cohen JI (eds) Fields Virology, vol 2, 7th edn. Lippincott Williams & Wilkins, pp 513–572
6. Decker LL, Shankar P, Khan G, Freeman RB, Dezube BJ, Lieberman J, Thorley-Lawson DA (1996) The Kaposi sarcoma-associated herpesvirus (KSHV) is present as an intact latent genome in KS tissue but replicates in the peripheral blood mononuclear cells of KS patients. J Exp Med 184:283–288. https://doi.org/10.1084/jem.184.1.283
7. Sun R, Lin SF, Staskus K, Gradoville L, Grogan E, Haase A, Miller G (1999) Kinetics of Kaposi's sarcoma-associated herpesvirus gene expression. J Virol 73:2232–42. https://doi.org/10.1128/jvi.73.3.2232-2242.1999
8. Jenner RG, Alba MM, Boshoff C, Kellam P (2001) Kaposi's sarcoma-associated herpesvirus latent and lytic gene expression as revealed by DNA arrays. J Virol 75:891–902. https://doi.org/10.1128/jvi.75.2.891-902.2001
9. Arias C, Weisburd B, Stern-Ginossar N, Mercier A, Madrid AS, Bellare P, et al. KSHV 2.0: A Comprehensive Annotation of the

Kaposi's Sarcoma-Associated Herpesvirus Genome Using Next-Generation Sequencing Reveals Novel Genomic and Functional Features. PLoS Pathog 2014;10:1003847. https://doi.org/10.1371/journal.ppat.1003847.
10. Nabiee R, Syed B, Castano JR, Lalani R, Totonchy JE. An update of the virion proteome of kaposi sarcoma-associated herpesvirus. Viruses 2020;12. https://doi.org/10.3390/v12121382.
11. Zhu FX, Chong JM, Wu L, Yuan Y. Virion Proteins of Kaposi's Sarcoma-Associated Herpesvirus. J Virol 2005;79:800. https://doi.org/10.1128/JVI.79.2.800-811.2005.
12. Butnaru M, Gaglia MM. The kaposi's sarcoma-associated herpesvirus protein orf42 is required for efficient virion production and expression of viral proteins. Viruses 2019;11. https://doi.org/10.3390/v11080711.
13. Liang Q, Wei D, Chung B, Brulois KF, Guo C, Dong S, et al. Novel Role of vBcl2 in the Virion Assembly of Kaposi's Sarcoma-Associated Herpesvirus. J Virol 2018;92. https://doi.org/10.1128/JVI.00914-17.
14. McGeoch DuncanJ, Davison AJ. The Molecular Evolutionary History of the Herpesviruses. Origin and Evolution of Viruses 1999:441–65. https://doi.org/10.1016/B978-012220360-2/50018-0.
15. Longnecker R, Neipel F. Introduction to the human γ-herpesviruses. Human Herpesviruses: Biology, Therapy, and Immunoprophylaxis 2007:341–59. https://doi.org/10.1017/CBO9780511545313.023.
16. Yanagi Y, Abdullah Al Masud HM, Watanabe T, Sato Y, Goshima F, Kimura H, et al. Initial Characterization of the Epstein–Barr Virus BSRF1 Gene Product. Viruses 2019;11. https://doi.org/10.3390/V11030285.
17. Nozawa N, Daikoku T, Koshizuka T, Yamauchi Y, Yoshikawa T, Nishiyama Y. Subcellular Localization of Herpes Simplex Virus Type 1 UL51 Protein and Role of Palmitoylation in Golgi Apparatus Targeting. J Virol 2003;77:3204–16. https://doi.org/10.1128/JVI.77.5.3204-3216.2003.
18. Albecka A, Owen DJ, Ivanova L, Brun J, Liman R, Davies L, et al. Dual Function of the pUL7-pUL51 Tegument Protein Complex in Herpes Simplex Virus 1 Infection. J Virol 2017;91. https://doi.org/10.1128/JVI.02196-16.
19. Masud HMA Al, Yanagi Y, Watanabe T, Sato Y, Kimura H, Murata T. Epstein-Barr Virus BBRF2 Is Required for Maximum Infectivity. Microorganisms 2019;7. https://doi.org/10.3390/MICROORGANISMS7120705.
20. Watanabe T, Nishimura M, Izumi T, Kuriyama K, Iwaisako Y, Hosokawa K, et al. Kaposi's Sarcoma-Associated Herpesvirus ORF66 Is Essential for Late Gene Expression and Virus Production via Interaction with ORF34. J Virol 2020;94. https://doi.org/10.1128/jvi.01300-19.
21. Brulois KF, Chang H, Lee AS-Y, Ensser A, Wong L-Y, Toth Z, et al. Construction and Manipulation of a New Kaposi's Sarcoma-Associated Herpesvirus Bacterial Artificial Chromosome Clone. J Virol 2012;86:9708–20. https://doi.org/10.1128/JVI.01019-12/SUPPL_FILE/ZJV999096466SO1.PDF.
22. Nishimura M, Watanabe T, Yagi S, Yamanaka T, Fujimuro M. Kaposi's sarcoma-associated herpesvirus ORF34 is essential for late gene expression and virus production. Sci Rep 2017;7. https://doi.org/10.1038/S41598-017-00401-7.
23. Wakao K, Watanabe T, Takadama T, Ui S, Shigemi Z, Kagawa H, et al. Sangivamycin induces apoptosis by suppressing Erk signaling in primary effusion lymphoma cells. Biochem Biophys Res Commun 2014;444:135–40. https://doi.org/10.1016/J.BBRC.2014.01.017.
24. Watanabe T, Nakamura S, Ono T, Ui S, Yagi S, Kagawa H, et al. Pyrrolidinium fullerene induces apoptosis by activation of procaspase-9 via suppression of Akt in primary effusion lymphoma. Biochem Biophys Res Commun 2014;451:93–100. https://doi.org/10.1016/J.BBRC.2014.07.068.
25. Roller RJ, Fetters R. The Herpes Simplex Virus 1 UL51 Protein Interacts with the UL7 Protein and Plays a Role in Its Recruitment into the Virion. J Virol 2015;89:3112–22. https://doi.org/10.1128/JVI.02799-14.
26. Erales J, Coffino P. Ubiquitin-independent proteasomal degradation. Biochimica et Biophysica Acta (BBA) - Molecular Cell Research 2014;1843:216–21. https://doi.org/10.1016/J.BBAMCR.2013.05.008.
27. Sander G, Konrad A, Thurau M, Wies E, Leubert R, Kremmer E, et al. Intracellular Localization Map of Human Herpesvirus 8 Proteins. J Virol 2008;82:1908–22. https://doi.org/10.1128/jvi.01716-07.
28. Awazawa R, Utsumi D, Katano H, Awazawa T, Miyagi T, Hayashi K, et al. High Prevalence of Distinct Human Herpesvirus 8 Contributes to the High Incidence of Non-acquired Immune Deficiency Syndrome-Associated Kaposi's Sarcoma in Isolated Japanese Islands. Journal of Infectious Diseases 2017;216:850–8. https://doi.org/10.1093/infdis/jix424.
29. Karsten Tischer B, Smith GA, Osterrieder N. En passant mutagenesis: A Two Markerless red recombination system. Methods in Molecular Biology 2010;634:421–30. https://doi.org/10.1007/978-1-60761-652-8_30.
30. Xu X, Guo Y, Fan S, Cui P, Feng M, Wang L, et al. Attenuated phenotypes and analysis of a herpes simplex virus 1 strain with partial deletion of the UL7, UL41 and LAT genes. Virol Sin 2017;32:404–14. https://doi.org/10.1007/S12250-017-3947-1/METRICS.
31. Roller RJ, Haugo AC, Yang K, Baines JD. The Herpes Simplex Virus 1 UL51 Gene Product Has Cell Type-Specific Functions in Cell-to-Cell Spread. J Virol 2014;88:4058–68. https://doi.org/10.1128/jvi.03707-13.
32. Oda S, Arii J, Koyanagi N, Kato A, Kawaguchi Y. The Interaction between Herpes Simplex Virus 1 Tegument Proteins UL51 and UL14 and Its Role in Virion Morphogenesis. J Virol 2016;90:8754. https://doi.org/10.1128/JVI.01258-16.